Available online at www.HEFJournal.org

HUMAN, EARTH AND FUTURE
Ital Publication

ISSN: 2785-2997

Journal of Human, Earth, and Future

Vol. 6, No. 1, March, 2025

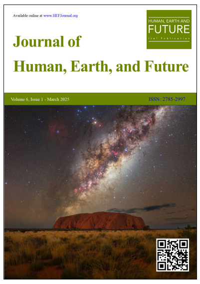

Effects of Hardwood Biomass Variability on Biochar Properties: Insights from Wood Waste Utilization

Saowanee Wijitkosum [1*], Thavivongse Sriburi [2]

[1] *Environmental Research Institute, Chulalongkorn University, Bangkok, 10330, Thailand.*

[2] *Pa-deng Biochar Research Center, Phetchaburi, 76170, Thailand.*

Received 24 October 2024; Revised 19 December 2024; Accepted 15 January 2025; Published 01 March 2025

Abstract

Wood is an abundant and renewable resource with considerable potential for upcycling into high-value products such as biochar, thereby facilitating the conversion of waste into useful materials. The structural and compositional diversity among wood species significantly influences the properties of the resulting biochar. This study aimed to investigate the properties of biochar derived from five distinct hardwood species, all sourced from the same tropical region and produced under standardized pyrolysis conditions using a patented furnace. The hardwood species examined were Leucaena (*Leucaena leucocephala* (Lamk.) de Wit.), paper flower climber (*Getonia floribunda* (Roxb.) Lam.), rain tree (*Samanea saman* (Jacq.) Merr.), climbing wattle (*Albizia myriophylla* Benth.), and Siamese blachia (*Blachia siamensis* Gagnep.). The investigation focused on fundamental properties of the biochar, including morphology, elemental composition (C, H, N, O), water-holding capacity, aromaticity (H/C ratio), polarity (O/C and (O+N)/C ratios), and the C/N ratio. Results indicated that all five biochar types were of high quality, with carbon contents ranging from 66.64% to 84.76%, a high degree of aromaticity (H/C < 0.7), low polarity, and enhanced stability. The biochars exhibited a range of pore structures from macropores to mesopores, with pore volumes of 0.010–0.074 cm^3/g and specific surface areas ranging from 2.92 m^2/g to 144.59 m^2/g. These structural attributes influence their water-holding capacities; however, the relationships among polarity, pore volume, pore size, and water-holding capacity remain unresolved. The findings highlighted substantial variability in the properties and morphology of the biochars, despite their production under identical conditions. This variability underscores the need for further in-depth studies to elucidate the factors governing biochar properties and to enable the tailoring of biochar for specific applications.

Keywords: Hardwood; Biochar; Upcycling; Lignocellulosic Biomass; Tropical Wood; Water-Holding Capacity.

1. Introduction

In recent years, addressing climate change has become a critical global challenge, necessitating strategies that simultaneously mitigate carbon emissions and enhance carbon sequestration. In this context, the land-use sector has emerged as a key area for intervention, with biochar gaining prominence as a promising material to support both direct and indirect climate policies [1]. Biochar is a stable carbon-rich solid material produced through the pyrolysis of biomass at the temperature range of 300°C to 700°C [2, 3], offering a dual benefit: it not only serves as a carbon sink but also enhances soil quality and agricultural productivity [4, 5]. These attributes position biochar as a multifunctional tool for addressing pressing environmental challenges.

* Corresponding author: saowanee.w@chula.ac.th

http://dx.doi.org/10. 28991/HEF-2025-06-01-02

The efficacy of biochar lies in its distinctive physicochemical properties, including its diverse pore structures [6, 7], surface functional groups [8], interfacial reactions [9], and liming capacity [10]. These characteristics make it suitable for various applications, such as improving soil fertility and enhancing crop yields [11, 12], sequestering carbon [13], and reducing greenhouse gas emissions [14, 15]. Biochar can be produced from a wide range of biomass sources, encompassing both wooden and non-wooden feedstocks [9, 16, 17]. Recent studies have extensively documented the significant influence of feedstock type and pyrolysis conditions on biochar properties [18-20]. Among the various feedstocks, wood biomass stands out due to its high lignin content, anisotropic porous structure, and rich carbon composition [19, 21]. However, the inherent variability in wood properties—driven by factors such as species, age, growth conditions, and geographical location—poses challenges in optimizing biochar production and tailoring its properties for specific applications [22, 23].

Wood biomass is a particularly attractive feedstock for biochar production due to its abundant availability, especially from underutilized sources such as pruning waste and residues from primary timber processing [24, 25]. Tropical hardwoods, in particular, represent an untapped resource with considerable significant potential for upcycling. These hardwoods exhibit diverse structural and compositional characteristics, including variations in cellulose (40–60%), hemicellulose (20–40%), and lignin (10–24%) content [26, 27]. Moreover, their highly porous structure spans a scale from the nanoscale within cell walls to the macroscale [28]. Notably, low-density wood generally contains a greater number of pores compared to high-density wood [29, 30]. For instance, the fixed carbon content of wood biomass varies significantly, ranging from 15.2% in beech wood [31] to 16.35% in lamtoro wood [32] and up to 35% in *Pinus pinaster* [33]. This variability underscores the necessity of systematic research to elucidate how different wood types influence biochar properties under controlled pyrolysis conditions [34].

A meta-analysis of the literature reveals that the physical and chemical properties of biochar are critical determinants of its suitability for various applications [35-37]. For example, Sun et al. [38] demonstrated that biochar-derived dissolved organic matter can stimulate microbial activity and promote plant growth. Similarly, Zhang et al. [39] highlighted that the hydrogen, nitrogen, and oxygen content significantly affects the water-holding capacity of biochar. Numerous studies have shown that both feedstock type and pyrolysis temperature substantially influence biochar characteristics [40, 41]. For instance, Huang et al. [40] and Zhang et al. [42] illustrated that variations in feedstock composition and pyrolysis conditions result in distinct chemical and physical properties of biochar. The conversion mechanism of biomass to biochar involves temperature-dependent intra- and intermolecular rearrangements, which are further modulated by the lignocellulosic composition of the biomass feedstock [43, 44]. Consequently, pyrolyzing different biomass types under identical conditions often yields biochar with highly variable properties [45–48].

Although correlations between pyrolysis temperature, feedstock properties, and biochar characteristics have been established [49-51], the literature reveals conflicting findings, particularly regarding wood-based biochar. For instance, higher pyrolysis temperatures generally increase the surface area and carbon content of biochar while reducing its nitrogen content [5, 52, 53]. Contradictory findings exist concerning nitrogen dynamics [43, 54]. Shaaban et al. [55] reported a decrease in the specific surface area of rubber wood biochar from 1.8 m^2/g to 1.4 m^2/g as the pyrolysis temperature rose from 300°C to 400°C. Furthermore, while biochar is typically alkaline, the pH range of wood-derived biochar can vary significantly, influenced by its ash content and pyrolysis conditions [56–58]. Additionally, there remains significant uncertainty surrounding the optimal adjustment of production conditions and biomass feedstocks to tailor biochar properties for specific applications [14, 47].

These inconsistencies underscore the inherent complexity of the pyrolysis process and highlight the need for further systematic research to optimize biochar properties for targeted applications. Tropical regions, characterized by high biodiversity and a wide variety of wood species, present a unique opportunity to investigate the potential of hardwoods as biochar feedstocks. However, most studies have focused on temperate regions, leaving a significant knowledge gap concerning tropical hardwoods [36]. Additionally, the use of cost-effective, locally fabricated biochar production technologies remains underexplored, despite their potential to enhance resource utilization and sustainability in tropical contexts [45]. Bridging these gaps is essential to advance biochar research and maximize its environmental and agricultural benefits. This study addresses these challenges by analyzing the physical structure and preliminary chemical properties of biochar derived from five types of tropical hardwood biomass. These feedstocks, sourced from the same geographical region, were pyrolyzed under uniform conditions using a locally fabricated, cost-effective biochar furnace. By focusing on tropical hardwoods and employing standardized production parameters, this research aims to provide new insights into the relationship between feedstock variability and biochar properties. Ultimately, the findings aim to contribute to the development of tailored biochar applications for agriculture and environmental management while promoting the sustainable utilization of underutilized wood resources.

2. Material and Methods

2.1. Hardwood Feedstock Preparation and Analysis

This study utilizes various types of hardwood commonly found in rural areas of Thailand as feedstock for pyrolysis. These hardwoods, primarily wood scraps resulting from pruning activities, are representative of underutilized biomass resources. Five species were selected for this study: Leucaena (*Leucaena leucocephala* (Lamk.) de Wit.), paper flower climber (*Getonia floribunda* (Roxb.) Lam.), rain tree (*Samanea saman* (Jacq.) Merr.), climbing wattle (*Albizia myriophylla* Benth.), and Siamese blachia (*Blachia siamensis* Gagnep.).

Hardwoods, systematically classified as angiosperms, are characterized by their complex and heterogeneous structures. Structural variations in hardwood result in differences in its properties, which are influenced by several factors, including the specific part of the tree (e.g., root, stem, or branch), environmental conditions during formation (e.g., microclimate), position within the stem (radial or longitudinal), and species-specific characteristics, both within and between species [59]. In this study, all hardwood feedstocks were grown in the same geographical region and collected from the Pa Deng subdistrict, located in the southwestern region of Kaeng Krachan National Park, Thailand (Figure 1). The five hardwood species analyzed, with samples collected exclusively from branches, are illustrated in Figure 2.

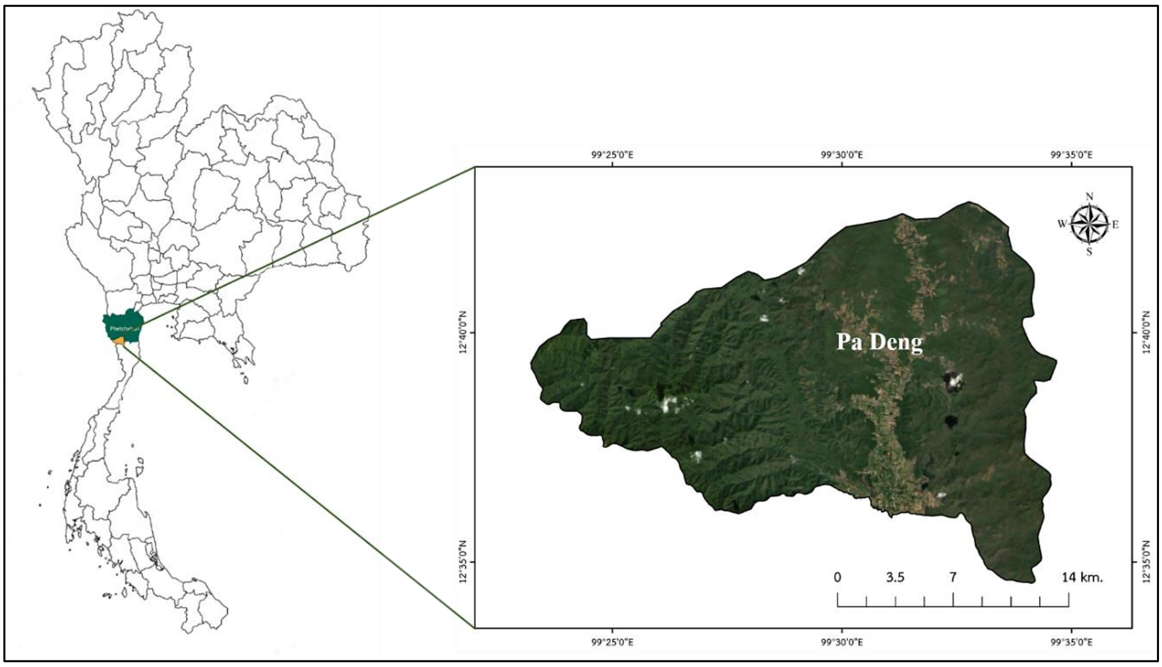

Figure 1. The Study Area

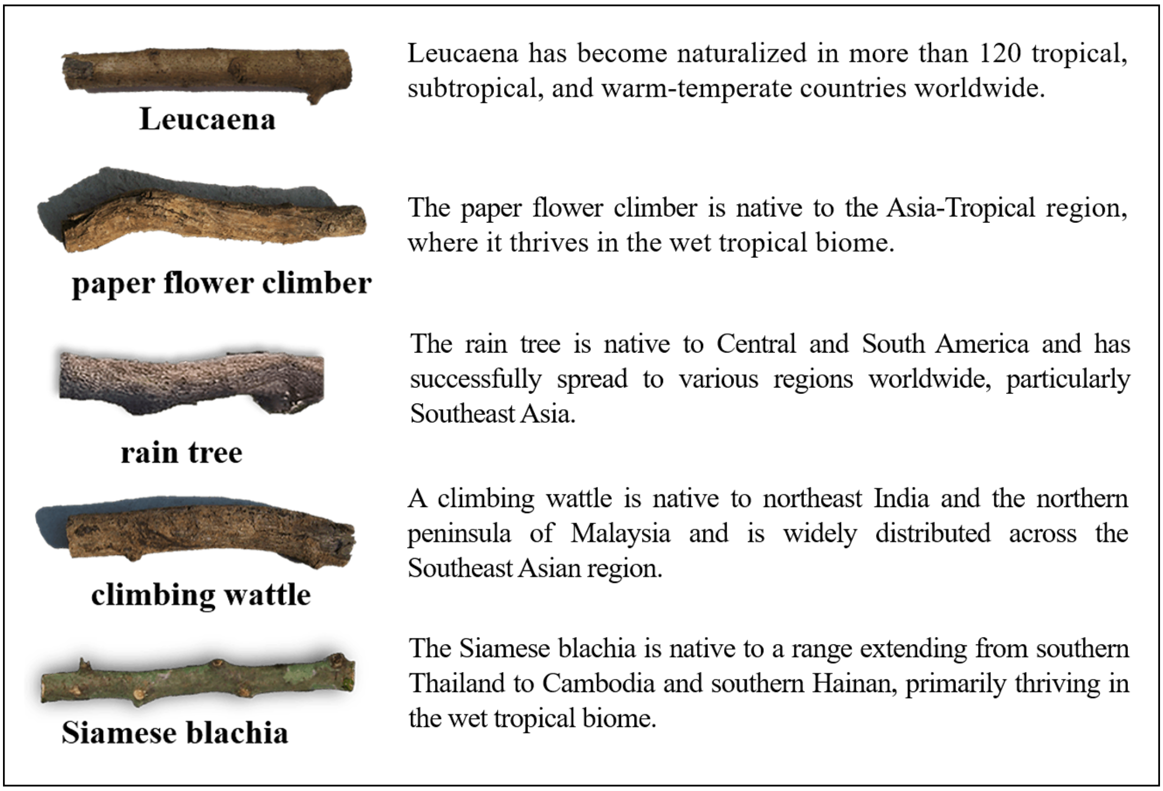

Figure 2. Five Types of Hardwood Used in the Study

The varying elemental compositions of different woody biomass types influence their pyrolysis behavior and the distribution of pyrolysis products [58, 60]. In this study, the five feedstock samples were ground and subjected to ultimate analysis to determine their carbon (C), hydrogen (H), and nitrogen (N) contents. The analysis adhered to ASTM D5373-16 standards and was conducted using an elemental analyzer (LECO Truspec CHN analyzer) under controlled conditions (950, 850°C, O_2 (HP), and He (UHP) [36, 61]. In accordance with ASTM protocols, the oxygen (O) content was calculated by subtracting the combined percentages of ash, C, H, and N from 100% [41]. Additionally, the O/C, H/C, (O+N)/C, and C/N ratios were computed to provide further insights into the elemental composition and the potential behavior of the feedstocks during the pyrolysis process [62].

2.2. Biochar Production

The hardwood feedstocks were uniformly cut into lengths of approximately 10–12 inches using a machine and subsequently air-dried for two days prior to pyrolysis. To ensure comparability of results, all five feedstocks underwent pyrolysis under identical and carefully controlled temperature and time conditions. The pyrolysis was conducted using the Controlled Temperature Biochar Retort for Slow Pyrolysis Process (CTBRSPP; patent number 50528) at a temperature range of 450–500°C for a duration of 4.30 hours. The biochar production methodology and its corresponding property analysis procedures are comprehensively illustrated in Figure 3.

The CTBRSPP has been developed since 2009 for the standardized production of high-quality biochar, with its patent filed in 2011 and granted in 2016. The design of the CTBRSPP emphasizes cost-effectiveness, ease of construction using locally available materials and equipment, and the ability for diverse feedstocks, including agricultural residues and wood wastes. The system's construction comprises an outer furnace made of two cement rings with a cement lid, a biochar retort fabricated from a 200 L cylindrical steel drum equipped with a lockable lid and clamps, and a chimney constructed from a cement pipe. Farmers can construct this furnace for agricultural use at an estimated cost of $42–$50, with durability allowing for 50–60 uses.

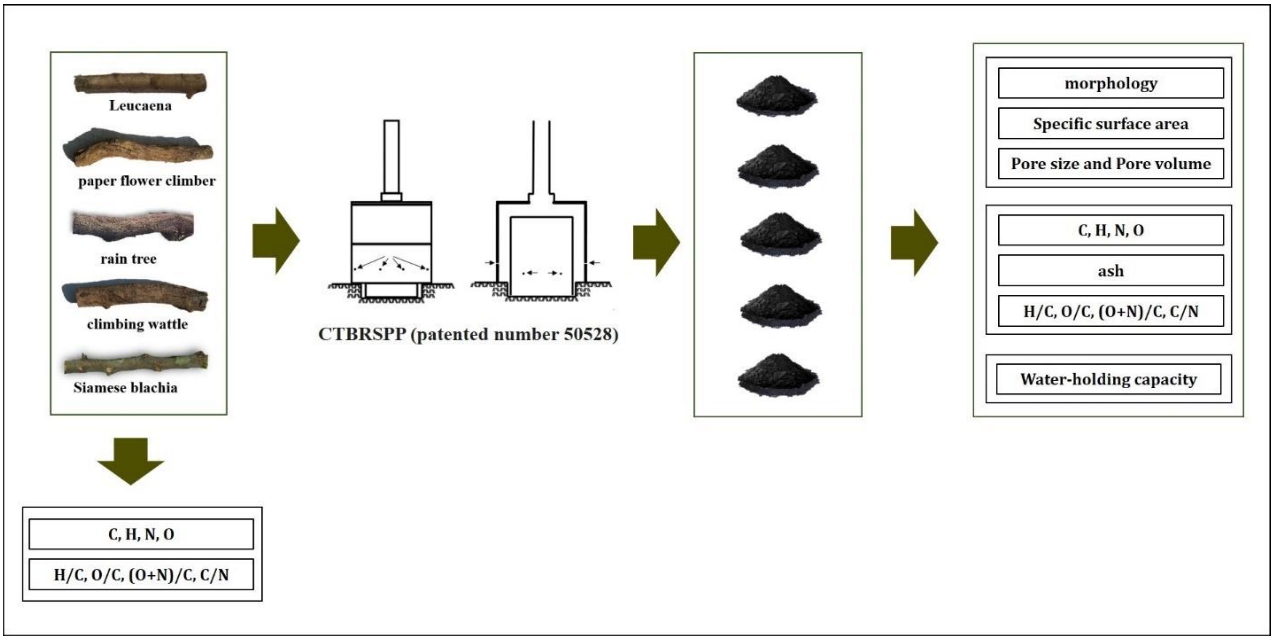

Figure 3. Biochar production and analyzed its properties

Pyrolysis conditions are meticulously controlled by regulating airflow into the system and managing temperature through strategically designed air intake holes. These holes, whose size, number, and placement were optimized through iterative trial-and-error testing, ensure the desired pyrolysis temperature is achieved to facilitate the release of syngas and volatiles into combustion. The number of air intake holes was twelve (each with a diameter of 2.5 cm) to determine the optimal airflow rate and combustion temperature. The effectiveness of the design has been validated through multiple studies, confirming its ability to produce biochar with desirable quality and properties suitable for agricultural applications. Temperature regulation in the retort is achieved by controlling the airflow into the kiln, which governs combustion within the space between the retort and the furnace. Temperature data were systematically recorded at various stages of the process from three locations: within the biochar retort, the outer retort, and the chimney tip. The outer furnace comprises two stacked cement pipes, with the lower pipe featuring eight holes to manage the temperature of the pyrolysis reaction. Additionally, the biochar retort, situated within the inner furnace, is equipped with four syngas outlet holes to ensure proper gas release during the process.

Upon completion of the pyrolysis process, the biochar samples were stored in airtight containers at room temperature to prevent contamination or alteration of their properties. The stored biochar was subsequently ground and sieved to achieve a uniform particle size of approximately 2–3 mm. These prepared samples were then subjected to physical property and elemental composition analyses without undergoing any additional treatments.

2.3. Biochar Analysis and Characterization

The analysis methods and parameters employed for biochar characterization adhered to the Standard Product Definitions and Product Testing Guidelines for Biochar Used in Soil [2, 41, 45]. The essential properties of biochar, particularly those relevant to its functionality in agricultural and environmental applications, were evaluated. Morphological characterization was conducted using a Scanning Electron Microscope (SEM; JEOL JEM-5410LV model) to observe surface structure and pore morphology. The physical properties, including specific surface area, pore size, and pore volume, were analyzed to assess the porosity and adsorption potential. The specific surface area of the biochar was measured using a surface area analyzer (Quantachrome Autosorb IQ-C-MP PFE, USA). Total pore volume and average pore diameter were determined using the Barrett–Joyner–Halenda (BJH) method [59].

Elemental analysis to determine the C, H, and N content was performed using a CHN analyzer in accordance with ASTM D5373-16. This method was also used to analyze the elemental composition of the feedstocks. The O content was calculated by mass difference, using the formula: [$\%O = 100 - (C\% + N\% + H\% + \text{ash } \%)$] [41, 63]. The elemental composition results were utilized to calculate the atomic ratios of H/C, O/C, and (O+N)/C, which are critical for classifying biochar and assessing its quality. These ratios provide insights into the aromaticity, polarity, and stability of the biochar [61]. Furthermore, these atomic ratios serve as indicators for predicting the carbon sequestration potential of biochar [62]. The water-holding capacity (WHC) of the biochar was evaluated using the equation: $WHC = (W_2 - W_1)/W_1$ [12, 64]. Dried biochar samples were initially weighed (W_1) and then immersed in water for 24 hr, and the wet weight (W_2) was measured using the vacuum method [5, 65]. The analysis of physical properties was conducted in three replicates, while the study of chemical properties was performed in four replicates to ensure the reliability and accuracy of the results.

3. Results and Discussion

3.1. Elemental Composition of Hardwood Feedstocks

The elemental composition of hardwood species, including C, H, N, and O, can vary significantly [26, 27, 45]. These variations are influenced by factors such as species type, growth conditions, age, and the relative proportions of cellular components, including cellulose, hemicellulose, and lignin [28, 34, 35]. The five hardwood species analyzed exhibited distinct differences in their C, H, and O contents, as presented in Table 1.

Table 1. Elemental compositions of different types of hardwood

Feedstock types	Ultimate analysis (%, air-dry basis)			
	C	H	N	O
Leucaena	43.76	6.17	0.15	49.92
paper flower climber	44.44	6.69	0.01	48.86
rain tree	42.69	6.21	0.01	51.09
climbing wattle	42.35	6.36	0.35	50.94
Siamese blachia	43.11	6.57	0.16	50.16

Remark: Data shown as the Mean with sample size = 4.0.

Carbon serves as the structural backbone of macromolecules such as cellulose, hemicelluloses, and lignin, which are integral to the structural integrity of wood [27, 41, 54]. Consequently, C constitutes a significant proportion of wood dry weight [28, 32]. The analysis indicated that the five hardwood biomass types exhibited relatively similar C contents, ranging from 42.35% to 44.44%, and H contents, ranging from 6.17% to 6.69%. Among the species analyzed, paper flower climber showed the highest C content (44.44%) and H content (6.69%), while climbing wattle recorded the lowest C content (42.35%). Variations in C content, typically ranging between 45–55% by weight, are primarily attributed to differences in lignin concentration, as lignin is a polymer with a high C density. Similarly, H content, which generally falls between 5–7% by weight, is influenced by the heterogeneity of hemicellulose [1, 40, 50, 59]. The O content across the five hardwood species varied between 48.86% and 51.09%. Oxygen is a major component of wood, often accounting for 35–50% by weight. Variations in O content are primarily due to differences in the cellulose and hemicellulose composition, as species with higher hemicellulose levels tend to have more O content because of the abundance of O-rich functional groups [36, 44, 54]. In this study, paper flower climbers demonstrated the lowest O content (48.86%) and N content (0.01%). Nitrogen content in wood is generally low, typically less than 1%, which aligns with the findings of this study, where N content in all five types of hardwood biochar ranged from 0.01% to 0.35%. However, certain hardwood species, particularly leguminous hardwoods with higher protein or nutrient levels in their tissue cells, may exhibit elevated N content [19, 59, 60]. For instance, Hu et al. [60] reported that Acacia had a higher N content (0.61%) compared to poplar wood (0.30%) and Ailanthus altissima (0.37%). In this study, Leucaena, rain tree, and climbing wattle were identified as leguminous hardwoods. Interestingly, rain tree showed a lower N content compared to Siamese Blachia, a non-leguminous species.

Table 2 presents the H/C, O/C, (O+N)/C, and C/N ratios for the five types of wood analyzed. These elemental ratios provide valuable insights into the structural characteristics, stability, reactivity, and suitability of wood for various applications.

Table 2. Ratio of elemental composition in different types of hardwood

Feedstock types	H/C	O/C	(O+N/C)	C/N
Leucaena	1.692	0.856	0.859	340.356
paper flower climber	1.806	0.825	0.825	5184.667
rain tree	1.746	0.898	0.898	4980.500
climbing wattle	1.802	0.902	0.909	141.167
Siamese blachia	1.829	0.873	0.876	314.344

The H/C ratio, indicative of a structure dominated by saturated characteristics, is typically associated with wood that has high cellulose or hemicellulose content [15, 27, 56]. In this study, the H/C ratios ranged from 1.692 to 1.829, with paper flower climber and climbing wattle displaying similar values. The highest H/C ratio was observed in Siamese blachia. The O/C ratio and (O+N)/C ratio reflect the level of O-containing functional groups in biomass, including woody structures. These ratios provide insights into the chemical composition, particularly the presence of O-rich functional groups such as hydroxyl, carbonyl, and carboxyl groups, which are integral components of polysaccharides and moisture in wood [8, 24, 63]. The O/C ratios were comparable across all wood types, ranging from 0.825 to 0.902, while the (O+N)/C ratios varied slightly, from 0.825 to 0.909. Climbing wattle exhibited the highest O/C and (O+N)/C ratios, whereas paper flower climber recorded the lowest values in both cases. In contrast, the C/N ratios demonstrated notable variability among the species. Paper flower climber and rain tree exhibited exceptionally high C/N ratios of 5184.667 and 4980.500, respectively, while climbing wattle recorded a significantly lower C/N ratio of 141.167. High C/N ratios are typically associated with lignin-rich wood, which is resistant to decomposition [26, 60, 62]. This characteristic makes such wood highly suitable for applications requiring decomposition resistance, such as biochar production [24, 65].

3.2. Physical Characterization of Hardwood Biochar

The thermochemical process significantly altered the morphology and characteristics of the lignocellulosic biomass, as presented in Table 3.

Table 3. Physical properties of different types of hardwood biochar

Biochar types	Average pore diameter (Å)	Specific surface area (m^2/g)	Total pore volume (cc/g)	Water holding capacity (%)
Leucaena	35.53	42.08	0.0374	38.26
Paper flower climber	143.10	2.92	0.0104	23.80
Rain tree	32.74	38.40	0.0396	45.82
Climbing wattle	163.10	3.67	0.0151	24.36
Siamese blachia	30.07	144.59	0.0739	25.08

Remark: Data shown as the Mean with sample size = 3.0.

The pyrolytic decomposition process induces significant structural changes in biomass feedstocks. At low temperatures (200–350°C), biomass undergoes dehydration, accompanied by the initial decomposition of hemicellulose and cellulose [2, 11, 18]. Hemicellulose decomposition predominantly occurs between 220–315°C, leaving approximately 20% of solid residue at 300°C. Cellulose decomposition becomes more pronounced in the temperature range of 315–400°C, and at temperatures exceeding 400°C, nearly all cellulose is pyrolyzed, leaving minimal solid residue [19, 22]. This initial stage of thermal decomposition releases volatile organic compounds from the carbon matrix, triggering the formation of biochar's pore structure and the development of rudimentary pores [31, 46, 53]. In contrast, lignin decomposition occurs gradually across the entire temperature range. Its slow degradation contributes to enhanced porosity and surface area, facilitated by material shrinkage and the formation of a more porous structure [6, 53, 55]. At temperatures above 450°C, the continued breakdown of lignin and residual organic materials further promotes pore development and increases the surface area of the biochar [21, 44, 48]. Consequently, biochar produced at these conditions exhibits highly variable and structurally complex surface morphologies.

The pore structure analysis of the five hardwood biochar types revealed a wide range of pore sizes, spanning from 30.07 Å to 163.10 Å. The formation and development of pores in biochar are influenced by the inherent porous architecture of the wood and its transformation during the pyrolysis process, both of which are critical to the biochar's physical and mechanical properties [3, 23, 59]. Hardwood exhibits a hierarchical porous architecture, ranging from macroscopic to supramolecular scales [24, 37], with porosity primarily influenced by its density [48]. Typically, hardwood is characterized by high density, ranging from 500 kg/m³ to 1,200 kg/m³, depending on the species [29, 57]. During pyrolysis, the compact structure of woody feedstock enhances cracking and supports the formation of porous networks. In addition, the compact and tightly arranged cellular fibers of hardwood result in biochar with fewer pores. This limited porosity is attributed to the high lignin concentration in hardwood, a complex organic polymer that contributes to its dense structure and restricts void formation during thermal decomposition [36, 28]. In contrast, lower-density woods, such as softwoods, generally contain higher cellulose content, which decomposes more readily during pyrolysis, leading to biochar with a more porous structure and larger pore formations [29, 57, 58]. Biochar derived from Leucaena, rain tree, and Siamese blachia exhibited pore sizes below 50 Å, classifying them as mesoporous according to the standards of the International Union of Pure and Applied Chemistry (IUPAC). This observation aligns with the general tendency of hardwood-derived biochar to predominantly exhibit mesoporous characteristics, attributed to its high-density structure [46]. Microporous structures can also develop at elevated pyrolysis temperatures (>500°C) [5, 6]. Conversely, biochar derived from climbing wattle and paper flower climber exhibited average pore diameters exceeding 100 Å, categorizing them as macroporous. The presence of macroporous structures in biochar has also been reported in specific hardwood species, such as eucalyptus [29] and poplar wood [30].

Biochar derived from wood often holds advantages over biochar from other feedstock types due to its relatively high lignin and cellulose contents, which contribute to an enhanced specific surface area [18, 34]. BET analysis revealed significant variability in the specific surface areas of the five hardwood biochar types. Among them, Siamese blachia biochar exhibited the highest specific surface area (144.59 m²/g), while paper flower climber and climbing wattle had substantially lower specific surface areas, measuring 2.92 m²/g and 3.67 m²/g, respectively. Biochar derived from Leucaena (42.08 m²/g) and rain tree (38.40 m²/g) displayed intermediate values. Additionally, the total pore volume ranged from 0.0104 cc/g to 0.0739 cc/g, reflecting the diversity in pore structures across the biochar types. The unique surface morphologies of the biochar samples were observed using a scanning electron microscope (SEM) (Figure 4). The five types of hardwood biochar displayed distinctly different surface structures, varying from uniform pores, as seen in Siamese blachia, to heterogeneous pores, as observed in Leucaena, paper flower climber, climbing wattle, and rain tree. The smallest pores were identified in Siamese blachia biochar, corresponding to its mesoporous structure, which also contributed to its highest surface area and pore volume. Conversely, large pores were observed in climbing wattle and paper flower climber, indicative of a macroporous structure, as evident in the SEM images.

Pore volume and pore diameter are critical parameters influencing the surface structure and functionality of biochar. Smaller pores generally contribute to a higher specific surface area due to their larger surface-to-volume ratio [34, 54, 55]. This trend was evident in biochar derived from paper flower climber, climbing wattle, and Siamese blachia, where a strong correlation between smaller pore sizes and higher specific surface areas was observed. These findings align with previous studies by Adhikari et al. [4], Li et al. [23], Leng et al. [37], and Wijitkosum [45]. However, contrasting results were reported by Shabir et al. [52], who observed that biochar derived from oak and pine exhibited smaller pores but did not correspondingly exhibit larger specific surface areas. The specific surface area and pore size distribution of biochar play pivotal roles in determining its adsorption kinetics and capacity, particularly for applications involving nutrient and water retention in soils. When applied to soil, biochar's porosity and surface area significantly influence its ability to adsorb nutrients and retain moisture [10, 38, 51]. In this study, the relatively low specific surface areas observed in some biochar samples may be attributed to the presence of residual inorganic materials, which likely obstructed or partially filled the pores. This hypothesis is supported by SEM images (Figure 4), which revealed evidence of pore blockage. These findings highlight the importance of feedstock selection and pyrolysis conditions in determining the structural properties of biochar. Optimizing these factors is essential for tailoring biochar for specific applications, particularly in agricultural and environmental management contexts.

The water-holding capacity (WHC) of biochar is influenced by key morphological factors, including surface area and pore structure [5, 11, 39]. In this study, biochar derived from paper flower climber and climbing wattle, characterized by macroporous structures, low total pore volumes, and low specific surface areas, exhibited relatively low WHC. These findings align with observations by Adhikari et al. [4] and Gondim et al. [5], who reported that biochar with macroporous structures generally demonstrates reduced WHC. However, contrasting findings have been reported in the literature [7, 30]. For example, Zhang & You [30] observed that biochar derived from poplar (Populus davidiana) with larger macropore diameters (1–40 µm) exhibited a higher WHC (69–72%) compared to pine wood biochar, which had smaller macropore diameters (1–10 µm) and a WHC of only 29%. Similarly, Shabir et al. [52] reported that biochar derived from oak wood with a pore size of 6.02 µm exhibited a WHC of 120%, whereas pine wood biochar with a slightly larger pore size of 6.38 µm demonstrated a lower WHC of 107%.

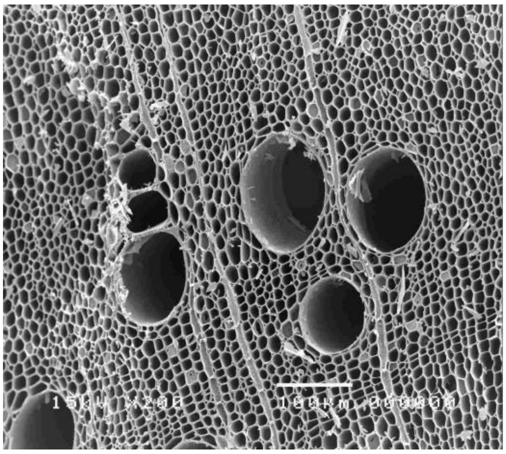

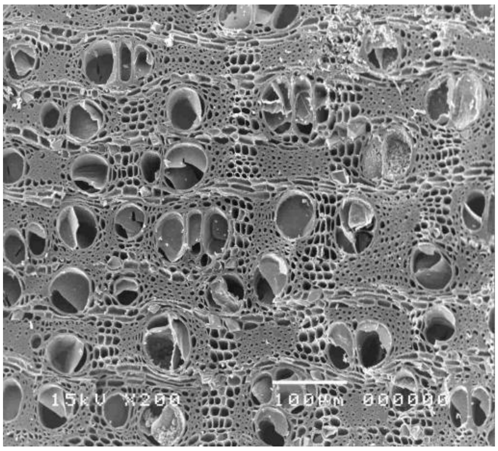

Leucaena **Paper flower climber**

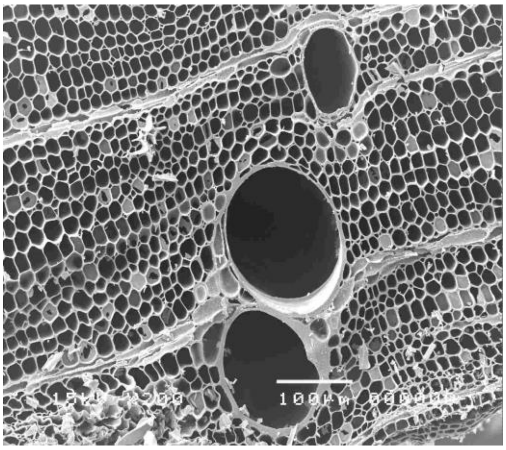

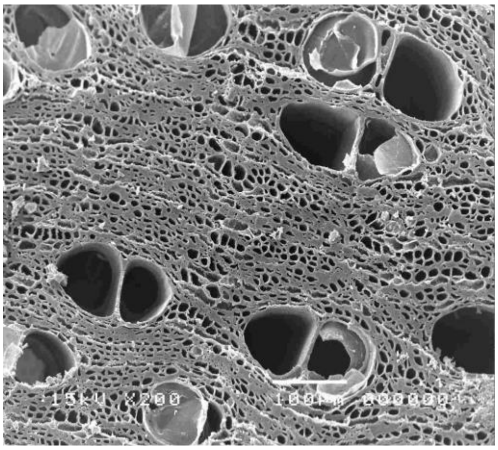

Rain tree **Climbing wattle**

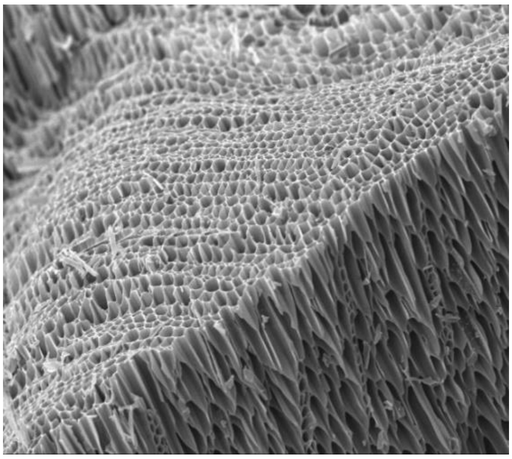

Siamese blachia

Figure 4. Scanning electron microscopy (SEM) images (200×) showing differences in the morphology of biochar derived from different hardwood feedstocks

Biochar with a larger surface area and greater porosity tends to exhibit higher WHC, primarily due to increased capillary forces and greater void volume for water retention [7]. Mesoporous structures, in particular, enhance WHC by facilitating surface contact and capillary action [4, 12, 18]. Larger pore volumes also improve WHC by providing additional space for water storage; however, the effectiveness of this enhancement depends on the distribution and connectivity of the pores [5, 39]. Interestingly, despite Siamese blachia biochar having the largest surface area, highest pore volume, and smallest pore size (mesopores) among the samples, it exhibited low WHC. In contrast, rain tree biochar, with a slightly higher total pore volume but a smaller surface area and larger pore size, demonstrated a higher WHC compared to Leucaena biochar. These findings underscore the complexity and variability in the properties of wood-derived biochar and their impact on WHC, consistent with previous studies by Boraah et al. [25], Werdin et al. [29], and Wijitkosum [45].

Understanding the WHC of biochar and its complex relationship with biochar characteristics is essential for designing and applying biochar effectively. When considering biochar for soil amendment, the pore size distribution plays a critical role in determining its impact on soil properties. Excessive micropores, while beneficial for retaining water, can impede adequate aeration and drainage, potentially leading to waterlogging in the soil [9, 17]. Conversely, macropores, which can store larger volumes of water, are more prone to rapid drainage due to gravitational forces [3, 46]. Biochar with macroporous structures plays a pivotal role in improving soil aeration and facilitating water infiltration and root penetration. In contrast, mesopores offer a balance between water retention and drainage, helping to maintain optimal soil moisture levels [11, 51]. The interaction between pore size, pore volume, and specific surface area collectively determines the overall WHC of biochar, making these factors critical for tailoring biochar to specific agricultural and environmental applications.

3.3. Elemental Composition of Hardwood Biochar

During the pyrolysis process, the physical structure of biochar is established, alongside significant changes in its elemental composition. The results have shown that with the increasing contents of C and N while decreasing contents of H and O. The C, H, N and O content of the biochar samples changed upon pyrolysis are shown in Table 4.

Table 4. Elemental compositions of different types of hardwood biochar

Biochar types	Ultimate analysis (%, air-dry basis)			
	C	H	N	O
Leucaena	84.61	2.47	1.03	11.89
paper flower climber	74.56	3.23	1.20	21.01
rain tree	84.76	2.43	0.64	11.66
climbing wattle	66.64	3.77	1.00	28.59
Siamese blachia	82.33	1.37	0.78	13.73

Remark: Data shown as the Mean with sample size = 4.0.

The variation in C content after converting feedstock into biochar is primarily due to the pyrolysis process and the distinct chemical composition of the precursors. Although the hardwood feedstocks had similar C content, the pyrolysis process involves complex thermal and chemical reactions that significantly alter the C structure and its proportion in the resulting biochar. The C content of the five hardwood biochar samples ranged from 66.64% to 84.76%. Similar findings have been reported for biochar derived from various woody feedstocks, including Acacia nilotica bark [21], applewood [33], lamtoro wood [32], sawdust [47], and pine bark [58] [11, 22, 23]. Among the samples, rain tree exhibited the highest C content (84.76%), closely followed by Leucaena biochar (84.61%), while climbing wattle biochar displayed the lowest C content (66.64%). The increase in C content in biochar is attributed to the pyrolysis process, which decomposes volatile organic compounds and gases, including CO_2, CO, H_2O, and volatile hydrocarbons [10, 13, 49]. This decomposition also breaks bonds between carbon and functional groups present in the biomass, such as -OH, aliphatic C–O, and aliphatic C–H groups [2, 8, 19]. At higher pyrolysis temperatures, the removal of volatile matter is enhanced, leading to a higher concentration of aromatic structures, particularly when temperatures exceed 400 °C. This process converts most aliphatic C into aromatic C, resulting in a more stable aromatic ring structure at temperatures above 450 °C [2, 38, 51].

Biochar samples derived from Leucaena, rain tree, and Siamese blachia exhibited C contents exceeding 80%, accompanied by low H and O contents. The H content of the biochar samples varied, ranging from 1.37% to 3.77%, depending on the composition of their precursor biomass. Similarly, the O content of the five hardwood biochar samples ranged from 11.66% to 28.59%. The decomposition of cellulose and lignin during pyrolysis results in a gradual loss of H and O, particularly at temperatures below 400 °C [25, 44, 58]. At higher pyrolysis temperatures, between 400 °C and 600 °C, the H and O content exhibited a sharp decline due to enhanced thermal decomposition [3, 48]. In addition, the O content in wood-based biochar is influenced by ash content. Wood-based biochar typically contains lower total ash levels, with most of the ash composed of alkali and alkaline earth metal carbonates, which form during the ashing process [43, 61].

Nitrogen content exhibits significant variability during the pyrolysis process, with reports indicating that biochar can exhibit either higher or lower N levels compared to its feedstock [2, 11, 48, 49, 61]. Nitrogen in biomass primarily exists as part of proteins and other nitrogenous compounds and is less volatile than C-based gases [41, 42, 50]. Generally, biochar retains less N content than its feedstock due to the volatilization of nitrogenous compounds during pyrolysis, a trend particularly evident in biochar derived from woody biomass. However, several studies have reported an increase in N content in biochar, especially at higher pyrolysis temperatures (>450 °C), a trend also observed in this study. Here, the N content of biochar increased across all five hardwood samples, ranging from 0.64% to 1.20%. Biochar derived from Leucaena and climbing wattle exhibited similar N contents of 1.03% and 1.00%, respectively. This observation aligns with findings from studies on pine bark biochar [22], lamtoro wood biochar [32], and bamboo biochar [35]. During pyrolysis, N-containing organic compounds in biomass undergo thermal decomposition, generating N-rich compounds such as ammonia (NH_3), which may become integrated into the solid biochar matrix. While some nitrogen is released as gases, such as nitrogen oxides (NO_x), a portion is retained in heterocyclic structures or stable aromatic carbon frameworks within the biochar [16, 21, 63]. These structures are less volatile and more resistant to decomposition, contributing to an increased N concentration in the biochar. Despite this increase, N remained a minor component of the overall elemental composition in all five hardwood biochar samples.

Interestingly, while the paper flower climber exhibited the highest C content among the feedstocks, the biochar derived from the rain tree had the highest C content after pyrolysis, despite the rain tree feedstock initially having one of the lowest C contents. The elemental composition of each hardwood feedstock underwent significant fluctuations during the pyrolysis process, without adhering to a consistent trend. Notably, rain tree had the lowest N content and the highest O content in its feedstock form. However, after pyrolysis, the resulting rain tree biochar displayed the lowest N and O contents. Furthermore, rain tree exhibited the fourth highest H content both in its feedstock form and after conversion to biochar. These findings highlight the complex and dynamic nature of elemental transformations in hardwood biomass during pyrolysis, underscoring the influence of feedstock composition and pyrolysis conditions on the final properties of biochar.

3.4. Aromaticity, Polarity, and Longevity of Hardwood Biochar

The atomic ratios of H/C, O/C, and (O+N)/C are essential for understanding the aromaticity, stability, and polarity of biochar. These ratios provide critical insights into the chemical structure and functional groups of biochar, which are key to evaluating its aromaticity and polarity and subsequently determining its potential applications. In this study, all biochar samples derived from the different hardwood feedstocks exhibited a high degree of aromatization, characterized by well-developed fused aromatic ring structures. This is evidenced by their atomic H/C ratios, which were consistently below 0.7 (Figure 5).

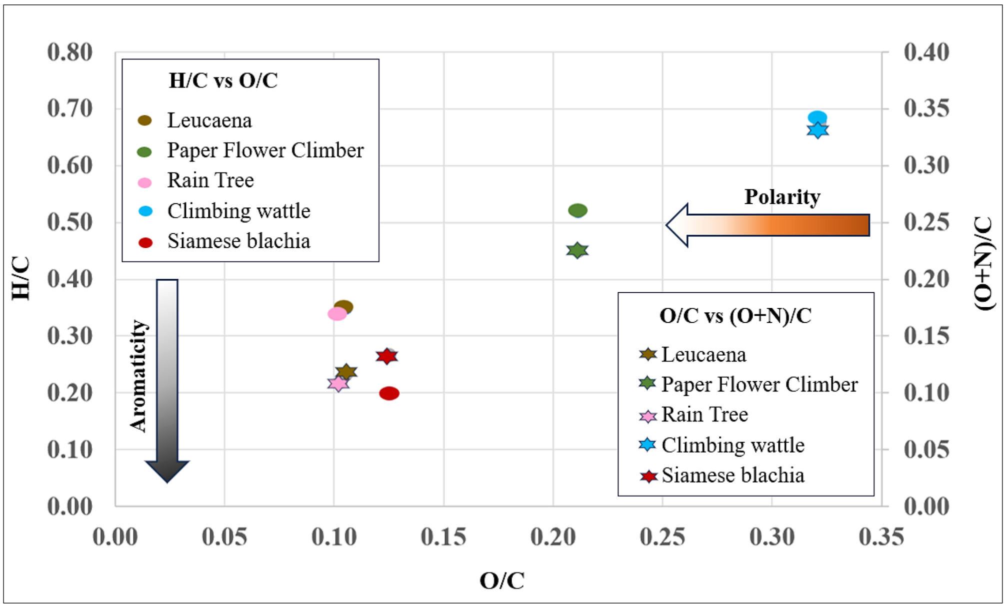

Figure 5. Correlations between the H/C and O/C ratios and between the O/C and (O+N)/C ratios for the five types of hardwood biochar

Compared to aliphatic structures, aromatic structures inherently have lower H content due to the dehydrogenation process that occurs during pyrolysis. This transformation converts aliphatic and less stable carbon forms into more stable aromatic structures [16, 24]. In this study, the H/C ratios of the five hardwood biochar samples ranged from 0.20 to 0.68, with Siamese blachia biochar exhibiting the lowest value and climbing wattle biochar the highest. The H/C ratios of Leucaena biochar (0.35) and rain tree biochar (0.34) were comparable. Generally, biochar derived from wood-based feedstocks tends to exhibit lower H/C ratios compared to biochar from other biomass types [45, 61]. The H/C ratio serves as a proxy for the degree of aromaticity and stability of biochar. The results indicated that Siamese blachia biochar had the highest aromaticity and stability due to its highly conjugated structure and reduced reactivity [16, 35].

The O/C ratio, indicative of oxidation and the presence of oxygenated functional groups, further characterizes biochar stability [8, 14, 35]. Similarly, the (O+N)/C ratio reflects the extent of heteroatom incorporation into the carbon matrix. Lower (O+N)/C ratios indicate the removal of these heteroatoms during pyrolysis, resulting in more condensed, graphitic-like carbon structures [41]. For instance, rain tree biochar, with an H/C ratio of 0.34, an O/C ratio of 0.10, and an (O+N)/C ratio of 0.11, exhibited high aromaticity and stability. Leucaena biochar displayed comparable ratios (H/C = 0.35, O/C = 0.11, (O+N)/C = 0.12). Interestingly, Siamese blachia biochar, despite its lowest H/C ratio (0.20), had higher O/C and (O+N)/C ratios than Leucaena and rain tree. Conversely, climbing wattle biochar showed the lowest aromaticity, retaining more aliphatic carbon and oxygenated functional groups, such as carboxyl, hydroxyl, and amine groups, which contributed to its higher polarity [14, 42, 56]. The O/C and (O+N)/C ratios of biochar are commonly used to describe its hydrophobicity and hydrophilicity, reflecting the chemical composition and functional groups present on the biochar surface. Oxygen is typically found in polar functional groups, such as carboxyl (-COOH), hydroxyl (-OH), and carbonyl (C=O), which are hydrophilic. Nitrogen-containing functional groups (e.g., amine (-NH2), nitro ($-NO_2$)) also contribute to hydrophilicity. Therefore, biochar with higher O and N contents typically contains more of these functional groups [14, 16], which play a critical role in defining its hydrophilic nature [8, 48, 60]. These functional groups undergo cracking and recombination during pyrolysis, significantly influencing biochar's specific surface area and surface chemistry [23, 47, 51]. These properties are largely determined by the feedstock's composition and the pyrolysis conditions [5, 8, 30].

Biochar with high O/C and (O+N)/C ratios exhibits hydrophilicity due to its abundant polar functional groups, which form H bonds with water molecules, enhancing water interaction. This facilitates stronger interactions with soil moisture, improving water retention properties [11, 39, 50]. Additionally, the surface functional groups increase active adsorption sites, enhancing the potential of biochar for environmental and agricultural applications [48]. In contrast, biochar dominated by aromatic structures with minimal polar functional groups exhibits hydrophobicity, reducing water interaction [8, 9, 63]. Thus, climbing wattle biochar showed higher hydrophilicity compared to others. Typically, biochar with O/C ratios below 0.2 is considered hydrophobic, aligning with high carbonization and aromaticity. In contrast, biochar with O/C ratios above 0.3 is considered hydrophilic, often derived from low-temperature pyrolysis with less condensed aromatic structures [62, 65]. In this study, climbing wattle biochar exhibited hydrophilicity. However, despite its hydrophilic nature, climbing wattle biochar had a low WHC, likely due to its small pore volume, limited surface area, and large pore size. By contrast, rain tree biochar, with the lowest O/C and (O+N)/C ratios, demonstrated the highest WHC. Siamese blachia biochar, despite its high N content, had a lower WHC compared to rain tree biochar. Paper flower climber biochar, though exhibiting greater hydrophilicity, had a lower WHC than biochars derived from Siamese blachia, Leucaena, and rain tree. These findings highlight the complexity of the thermal decomposition process during biomass-to-biochar conversion. They also corroborate findings by Godim et al. [5], Liu et al. [7], Adhikari et al. [12], and Zhang et al. [30], who emphasized that WHC in biochar is influenced by multiple factors and requires further investigation. Future studies should examine zeta potential, surface angularity, and inter-particle porosity to better understand its water retention and absorption characteristics of biochar.

The degree of aromaticity, as indicated by the H/C ratio, serves as a measure of biochar stability, reflecting hydrogen saturation in the carbon structure [31, 59]. However, the O/C ratio is considered more critical in influencing biochar stability, as reactive O-containing functional groups significantly impact its chemical stability [50, 56, 61]. This influences biochar's quality and phase distribution [60]. The O/C ratios of biochar derived from Leucaena, rain tree, and Siamese blachia indicated high stability and condensed carbon structures (O/C < 0.2), suggesting the absence of residual structures from the parent biomass [60]. Among these, rain tree biochar exhibited the highest stability, despite Siamese blachia biochar having the greatest aromaticity. The low O/C ratio of rain tree biochar suggests greater carbon stability, as O-containing groups are more reactive and prone to decomposition over time [41, 43, 59]. This is further supported by its lowest (O+N)/C ratio and highest C/N ratio. The C/N ratios of the five hardwood biochar samples ranged from 72.49 to 154.51. While wood-derived biochar has been reported to exhibit C/N ratios as high as 300 [2, 63], hardwood biochar generally has slightly lower C/N ratios than softwood biochar due to the higher nitrogen content in hardwood [1, 11, 40].

In terms of application, the H/C ratio of biochar is a reliable indicator of its capacity to reduce N_2O emissions, with a low H/C ratio linked to greater mitigation potential. Biochar with H/C ratios below 0.3 can reduce N_2O emissions by up to 73% [15]. Based on this criterion, Siamese blachia biochar demonstrates strong potential for greenhouse gas mitigation. The C/N ratio is another valuable metric for assessing biochar stability and its interactions with the environment, particularly in nutrient cycling, decomposition, soil health, and carbon sequestration [13, 17, 49]. This study revealed that rain tree biochar, with a C/N ratio of 154.51, exhibited the lowest decomposition rate, indicating high resistance to microbial degradation and greater potential for long-term carbon sequestration. In contrast, climbing wattle biochar, despite not having the lowest C/N ratio, showed the lowest stability, as reflected in its higher H/C, O/C, and (O+N)/C ratios.

4. Conclusion

Hardwood biomass is a promising feedstock for enhancing its utility by converting it into biochar. This study focused on biochar production from five types of local hardwood biomass—Leucaena, paper flower climber, rain tree, climbing wattle, and Siamese Blachia—using a patented furnace. Despite originating from the same geographic region, each hardwood species exhibited distinct characteristics. Pyrolysis under uniform conditions, at temperatures ranging from 450 to 500 °C, led to variations in the biochar properties produced from each type of wood. Initially, the carbon content of the five hardwood species ranged from 42.35% to 44.44%, but after thermal decomposition, the carbon content increased significantly, with some types displaying notable differences. All five types of hardwood biochar displayed diverse structural characteristics, including pore sizes ranging from mesopores to macropores and specific surface areas ranging from 2.92 m^2/g to 144.59 m^2/g. The thermal decomposition process significantly increased the carbon content while reducing the oxygen content in all biochar. Each type of biochar demonstrated high quality, with carbon contents exceeding 65%, an H/C ratio lower than 0.7, and an O/C ratio lower than 0.4. Among them, the climbing wattle biochar exhibited the lowest carbon content at 66.64%, along with lower stability and higher polarity compared to the other biochar. Conversely, the rain tree biochar and Leucaena biochar had the highest carbon contents of 84.76% and 84.61%, respectively, and were characterized by high aromaticity and stability, as indicated by their low H/C, O/C, and (O+N)/C ratios. In terms of potential applications, the findings suggest that all five types of hardwood biochar can be used as soil additives, with significant potential for climate change mitigation. Notably, this study highlights that pore size and pore volume, rather than polarity, are critical factors influencing the WHC of biochar. These results underscore the variability and complexity inherent in biochar derived from different wood types, emphasizing the heterogeneity in wood-based biochar characteristics.

5. Declarations

5.1. Author Contributions

Conceptualization, S.W.; methodology, S.W. and T.S.; formal analysis, S.W.; investigation, S.W. and T.S.; resources, T.S.; data curation, S.W.; writing—original draft preparation, S.W.; writing—review and editing, S.W.; visualization, S.W. All authors have read and agreed to the published version of the manuscript

5.2. Data Availability Statement

The data presented in this study are available in the article.

5.3. Funding

The authors received no financial support for the research, authorship, and/or publication of this article.

5.4. Institutional Review Board Statement

Not applicable.

5.5. Informed Consent Statement

Not applicable.

5.6. Declaration of Competing Interest

The authors declare that there are no conflicts of interest concerning the publication of this manuscript. Furthermore, all ethical considerations, including plagiarism, informed consent, misconduct, data fabrication and/or falsification, double publication and/or submission, and redundancies have been completely observed by the authors.

6. References

[1] Papageorgiou, A., Azzi, E. S., Enell, A., & Sundberg, C. (2021). Biochar produced from wood waste for soil remediation in Sweden: Carbon sequestration and other environmental impacts. Science of the total environment, 776, 145953. doi:10.1016/j.scitotenv.2021.145953.

[2] Luo, L., Xu, C., Chen, Z., & Zhang, S. (2015). Properties of biomass-derived biochars: Combined effects of operating conditions and biomass types. Bioresource Technology, 192, 83-89. doi:10.1016/j.biortech.2015.05.054.

[3] He, M., Xu, Z., Sun, Y., Chan, P. S., Lui, I., & Tsang, D. C. W. (2021). Critical impacts of pyrolysis conditions and activation methods on application-oriented production of wood waste-derived biochar. Bioresource Technology, 341, 125811. doi:10.1016/j.biortech.2021.125811.

[4] Adhikari, S., Moon, E., Paz-Ferreiro, J., & Timms, W. (2024). Comparative analysis of biochar carbon stability methods and implications for carbon credits. Science of the Total Environment, 914, 169607. doi:10.1016/j.scitotenv.2023.169607.

[5] Gondim, R. S., Muniz, C. R., Lima, C. E. P., & Santos, C. L. A. Dos. (2018). Explaining the water-holding capacity of biochar by scanning electron microscope images. Revista Caatinga, 31(4), 972–979. doi:10.1590/1983-21252018V31N420RC.

[6] Wang, L., Chen, L., Tsang, D. C. W., Guo, B., Yang, J., Shen, Z., Hou, D., Ok, Y. S., & Poon, C. S. (2020). Biochar as green additives in cement-based composites with carbon dioxide curing. Journal of Cleaner Production, 258, 120678. doi:10.1016/j.jclepro.2020.120678.

[7] Liu, Z., Dugan, B., Masiello, C. A., & Gonnermann, H. M. (2017). Biochar particle size, shape, and porosity act together to influence soil water properties. PLoS ONE, 12(6), 179079. doi:10.1371/journal.pone.0179079.

[8] Cervera-Mata, A., Aranda, V., Ontiveros-Ortega, A., Comino, F., Martín-García, J. M., Vela-Cano, M., & Delgado, G. (2021). Hydrophobicity and surface free energy to assess spent coffee grounds as soil amendment. Relationships with soil quality. Catena, 196, 104826. doi:10.1016/j.catena.2020.104826.

[9] Edeh, I. G., Mašek, O., & Buss, W. (2020). A meta-analysis on biochar's effects on soil water properties – New insights and future research challenges. Science of the Total Environment, 714, 136857. doi:10.1016/j.scitotenv.2020.136857.

[10] Weber, K., & Quicker, P. (2018). Properties of biochar. Fuel, 217, 240–261. doi:10.1016/j.fuel.2017.12.054.

[11] Huang, H., Cai, W. L., Zheng, Q., Chen, P. N., Huang, C. R., Zeng, Q. J., ... & Kushvaha, V. (2020). Gas permeability in soil amended with biochar at different compaction states. IOP Conference Series: Earth and Environmental Science, 463, 1, 012073. doi:10.1088/1755-1315/463/1/012073.

[12] Adhikari, S., Mahmud, M. A. P., Nguyen, M. D., & Timms, W. (2023). Evaluating fundamental biochar properties in relation to water holding capacity. Chemosphere, 328, 138620. doi:10.1016/j.chemosphere.2023.138620.

[13] Guo, S., Li, Y., Wang, Y., Wang, L., Sun, Y., & Liu, L. (2022). Recent advances in biochar-based adsorbents for CO_2 capture. Carbon Capture Science and Technology, 4, 100059. doi:10.1016/j.ccst.2022.100059.

[14] Wu, P., Singh, B. P., Wang, H., Jia, Z., Wang, Y., & Chen, W. (2023). Bibliometric analysis of biochar research in 2021: a critical review for development, hotspots and trend directions. Biochar, 5(1), 6. doi:10.1007/s42773-023-00204-2.

[15] Cayuela, M. L., Jeffery, S., & van Zwieten, L. (2015). The molar H: COrg ratio of biochar is a key factor in mitigating N2O emissions from soil. Agriculture, Ecosystems and Environment, 202, 135–138. doi:10.1016/j.agee.2014.12.015.

[16] Cao, Q., An, T., Xie, J., Liu, Y., Xing, L., Ling, X., & Chen, C. (2022). Insight to the physiochemical properties and DOM of biochar under different pyrolysis temperature and modification conditions. Journal of Analytical and Applied Pyrolysis, 166, 105590. doi:10.1016/j.jaap.2022.105590.

[17] Das, S., Mohanty, S., Sahu, G., Rana, M., & Pilli, K. (2021). Biochar: A Sustainable Approach for Improving Soil Health and Environment. Soil Erosion - Current Challenges and Future Perspectives in a Changing World. IntechOpen. doi:10.5772/intechopen.97136.

[18] Uroić Štefanko, A., & Leszczynska, D. (2020). Impact of Biomass Source and Pyrolysis Parameters on Physicochemical Properties of Biochar Manufactured for Innovative Applications. Frontiers in Energy Research, 8, 138. doi:10.3389/fenrg.2020.00138.

[19] Qiu, L., Li, C., Zhang, S., Wang, S., Li, B., Cui, Z., Tang, Y., & Hu, X. (2023). Distinct property of biochar from pyrolysis of poplar wood, bark, and leaves of the same origin. Industrial Crops and Products, 202, 117001. doi:10.1016/j.indcrop.2023.117001.

[20] Xu, W., Xu, H., Delgado-Baquerizo, M., Gundale, M. J., Zou, X., & Ruan, H. (2023). Global meta-analysis reveals positive effects of biochar on soil microbial diversity. Geoderma, 436, 116528. doi:10.1016/j.geoderma.2023.116528.

[21] Murtaza, G., Ahmed, Z., Usman, M., Iqbal, R., Zulfiqar, F., Tariq, A., & Ditta, A. (2024). Physicochemical properties and performance of non-woody derived biochars for the sustainable removal of aquatic pollutants: A systematic review. Chemosphere, 359. doi:10.1016/j.chemosphere.2024.142368.

[22] Tiwari, M., Dirbeba, M. J., Lehmusto, J., Yrjas, P., & Vinu, R. (2024). Analytical and applied pyrolysis of challenging biomass feedstocks: Effect of pyrolysis conditions on product yield and composition. Journal of Analytical and Applied Pyrolysis, 177, 106355. doi:10.1016/j.jaap.2024.106355.

[23] Li, X., Liu, N., Zhang, J., Sun, Z., Fu, S., Zhan, X., Yang, J., Zhou, R., Zhang, H., Liu, H., & Han, X. (2023). Pyrolysis temperature had effects on the physicochemical properties of biochar. Plant, Soil and Environment, 69(8), 363–373. doi:10.17221/444/2022-PSE.

[24] Jiao, H., Guo, X., Shu, F., Zhang, Q., Wu, W., Jin, Y., & Jiang, B. (2025). Structure-property-function relationships of wood-based activated carbon in energy and environment materials. Separation and Purification Technology, 353. doi:10.1016/j.seppur.2024.128607.

[25] Boraah, N., Chakma, S., & Kaushal, P. (2023). Optimum features of wood-based biochars: A characterization study. Journal of Environmental Chemical Engineering, 11(3), 109976. doi:10.1016/j.jece.2023.109976.

[26] Čabalová, I., Bélik, M., Kučerová, V., Jurczyková, T., & Bubeníková, T. (2023). Evaluation of Chemical and Morphological Properties of Spruce Wood Stored in the Natural Environment. Polymers, 15(24), 4734. doi:10.3390/polym15244734.

[27] K N, Y., T, P. D., P, S., S, K., R, Y. K., Varjani, S., AdishKumar, S., Kumar, G., & J, R. B. (2022). Lignocellulosic biomass-based pyrolysis: A comprehensive review. Chemosphere, 286, 131824. doi:10.1016/j.chemosphere.2021.131824.

[28] Ling, S., Kaplan, D. L., & Buehler, M. J. (2018). Nanofibrils in nature and materials engineering. Nature Reviews Materials, 3(4), 1–15. doi:10.1038/natrevmats.2018.16.

[29] Werdin, J., Fletcher, T. D., Rayner, J. P., Williams, N. S. G., & Farrell, C. (2020). Biochar made from low density wood has greater plant available water than biochar made from high density wood. Science of the Total Environment, 705, 135856. doi:10.1016/j.scitotenv.2019.135856.

[30] Zhang, J., & You, C. (2013). Water holding capacity and absorption properties of wood chars. Energy and Fuels, 27(5), 2643–2648. doi:10.1021/ef4000769.

[31] Guizani, C., Jeguirim, M., Valin, S., Peyrot, M., & Salvador, S. (2019). The Heat Treatment Severity Index: A new metric correlated to the properties of biochars obtained from entrained flow pyrolysis of biomass. Fuel, 244, 61–68. doi:10.1016/j.fuel.2019.01.170.

[32] Nurhadi, N., Rianda, S., Irawan, C., & Pramono, G. P. (2021). Biochar production investigation from pyrolysis of lamtoro wood as a coal blend for fuel substitution in steam power plants. IOP Conference Series: Earth and Environmental Science, 749(1), 12037. doi:10.1088/1755-1315/749/1/012037.

[33] Lataf, A., Jozefczak, M., Vandecasteele, B., Viaene, J., Schreurs, S., Carleer, R., Yperman, J., Marchal, W., Cuypers, A., & Vandamme, D. (2022). The effect of pyrolysis temperature and feedstock on biochar agronomic properties. Journal of Analytical and Applied Pyrolysis, 168, 105728. doi:10.1016/j.jaap.2022.105728.

[34] Jamal, M. U., & Fletcher, A. J. (2023). Design of Experiments Study on Scottish Wood Biochars and Process Parameter Influence on Final Biochar Characteristics. Bioenergy Research, 16(4), 2342–2355. doi:10.1007/s12155-023-10595-6.

[35] Sahoo, S. S., Vijay, V. K., Chandra, R., & Kumar, H. (2021). Production and characterization of biochar produced from slow pyrolysis of pigeon pea stalk and bamboo. Cleaner Engineering and Technology, 3, 100101. doi:10.1016/j.clet.2021.100101.

[36] Moya, R., Tenorio, C., Quesada-Kimzey, J., & Másis-Meléndez, F. (2024). Pyrogenic Carbonaceous Materials Production of Four Tropical Wood Produced by Slow Pyrolysis at Different Temperatures: Charcoal and Biochar Properties. Energies, 17(8), 1953. doi:10.3390/en17081953.

[37] Leng, L., Xiong, Q., Yang, L., Li, H., Zhou, Y., Zhang, W., Jiang, S., Li, H., & Huang, H. (2021). An overview on engineering the surface area and porosity of biochar. Science of the Total Environment, 763, 144204. doi:10.1016/j.scitotenv.2020.144204.

[38] Sun, Y., Xiong, X., He, M., Xu, Z., Hou, D., Zhang, W., Ok, Y. S., Rinklebe, J., Wang, L., & Tsang, D. C. W. (2021). Roles of biochar-derived dissolved organic matter in soil amendment and environmental remediation: A critical review. Chemical Engineering Journal, 424, 130387. doi:10.1016/j.cej.2021.130387.

[39] Zhang, H., Cheng, Y., Zhong, Y., Ni, J., Wei, R., & Chen, W. (2024). Roles of biochars' properties in their water-holding capacity and bound water evaporation: quantitative importance and controlling mechanism. Biochar, 6(1), 30. doi:10.1007/s42773-024-00317-2.

[40] Huang, H., Reddy, N. G., Huang, X., Chen, P., Wang, P., Zhang, Y., ... & Garg, A. (2021). Effects of pyrolysis temperature, feedstock type and compaction on water retention of biochar amended soil. Scientific Reports, 11(1), 7419. doi:10.1038/s41598-021-86701-5.

[41] Wijitkosum, S. (2023). Influence of Pyrolysis Temperature and Time on Biochar Properties and Its Potential for Climate Change Mitigation. Journal of Human, Earth, and Future, 4(4), 472–485. doi:10.28991/HEF-2023-04-04-07.

[42] Zhang, H., Chen, C., Gray, E. M., & Boyd, S. E. (2017). Effect of feedstock and pyrolysis temperature on properties of biochar governing end use efficacy. Biomass and Bioenergy, 105, 136–146. doi:10.1016/j.biombioe.2017.06.024.

[43] Tu, P., Zhang, G., Wei, G., Li, J., Li, Y., Deng, L., & Yuan, H. (2022). Influence of pyrolysis temperature on the physicochemical properties of biochars obtained from herbaceous and woody plants. Bioresources and Bioprocessing, 9(1), 131. doi:10.1186/s40643-022-00618-z.

[44] Hernandez-Mena, L. E., Pecora, A. A. B., & Beraldo, A. L. (2014). Slow pyrolysis of bamboo biomass: Analysis of biochar properties. Chemical Engineering Transactions, 37, 115–120. doi:10.3303/CET1437020.

[45] Wijitkosum, S. (2022). Biochar derived from agricultural wastes and wood residues for sustainable agricultural and environmental applications. International Soil and Water Conservation Research, 10(2), 335-341. doi:10.1016/j.iswcr.2021.09.006.

[46] Tomczyk, A., Sokołowska, Z., & Boguta, P. (2020). Biochar physicochemical properties: pyrolysis temperature and feedstock kind effects. Reviews in Environmental Science and Biotechnology, 19(1), 191–215. doi:10.1007/s11157-020-09523-3.

[47] Khater, E. S., Bahnasawy, A., Hamouda, R., Sabahy, A., Abbas, W., & Morsy, O. M. (2024). Biochar production under different pyrolysis temperatures with different types of agricultural wastes. Scientific Reports, 14(1), 2625. doi:10.1038/s41598-024-52336-5.

[48] He, D., Luo, Y., & Zhu, B. (2024). Feedstock and pyrolysis temperature influence biochar properties and its interactions with soil substances: Insights from a DFT calculation. Science of the Total Environment, 922, 171259. doi:10.1016/j.scitotenv.2024.171259.

[49] Almutairi, A. A., Ahmad, M., Rafique, M. I., & Al-Wabel, M. I. (2023). Variations in composition and stability of biochars derived from different feedstock types at varying pyrolysis temperature. Journal of the Saudi Society of Agricultural Sciences, 22(1), 25-34. doi:10.1016/j.jssas.2022.05.005.

[50] Wang, Y., Zeng, X., Li, Q., Jin, J., Xiao, S., Xu, X., & Ding, W. (2024). Surface functionalizing woody biochar with UV irradiation to promote adsorption of heavy metals. BioResources, 19(4), 7566–7590. doi:10.15376/biores.19.4.7566-7590.

[51] Al-Wabel, M. I., Hussain, Q., Usman, A. R. A., Ahmad, M., Abduljabbar, A., Sallam, A. S., & Ok, Y. S. (2018). Impact of biochar properties on soil conditions and agricultural sustainability: A review. Land Degradation and Development, 29(7), 2124–2161. doi:10.1002/ldr.2829.

[52] Shabir, R., Li, Y., Zhang, L., & Chen, C. (2023). Biochar surface properties and chemical composition determine the rhizobial survival rate. Journal of Environmental Management, 326, 116594. doi:10.1016/j.jenvman.2022.116594.

[53] Sbizzaro, M., César Sampaio, S., Rinaldo dos Reis, R., de Assis Beraldi, F., Medina Rosa, D., Maria Branco de Freitas Maia, C., Saramago de Carvalho Marques dos Santos Cordovil, C., Tillvitz do Nascimento, C., Antonio da Silva, E., & Eduardo Borba, C. (2021). Effect of production temperature in biochar properties from bamboo culm and its influences on atrazine adsorption from aqueous systems. Journal of Molecular Liquids, 343, 117667. doi:10.1016/j.molliq.2021.117667.

[54] Arous, S., Koubaa, A., Bouafif, H., Bouslimi, B., Braghiroli, F. L., & Bradai, C. (2021). Effect of pyrolysis temperature and wood species on the properties of biochar pellets. Energies, 14(20), 6529. doi:10.3390/en14206529.

[55] Shaaban, A., Se, S. M., Dimin, M. F., Juoi, J. M., Mohd Husin, M. H., & Mitan, N. M. M. (2014). Influence of heating temperature and holding time on biochars derived from rubber wood sawdust via slow pyrolysis. Journal of Analytical and Applied Pyrolysis, 107, 31–39. doi:10.1016/j.jaap.2014.01.021.

[56] Gezahegn, S., Sain, M., & Thomas, S. C. (2019). Variation in feedstock wood chemistry strongly influences biochar liming potential. Soil Systems, 3(2), 1–16. doi:10.3390/soilsystems3020026.

[57] Rizwan, M., Murtaza, G., Zulfiqar, F., Moosa, A., Iqbal, R., Ahmed, Z., Irshad, S., Khan, I., Li, T., Chen, J., Zhang, M., Siddique, K. H. M., Leng, L., & Li, H. (2023). Sustainable manufacture and application of biochar to improve soil properties and remediate soil contaminated with organic impurities: a systematic review. Frontiers in Environmental Science, 11, 1277240. doi:10.3389/fenvs.2023.1277240.

[58] Domingues, R. R., Trugilho, P. F., Silva, C. A., De Melo, I. C. N. A., Melo, L. C. A., Magriotis, Z. M., & Sánchez-Monedero, M. A. (2017). Properties of biochar derived from wood and high-nutrient biomasses with the aim of agronomic and environmental benefits. PLoS ONE, 12(5), 176884. doi:10.1371/journal.pone.0176884.

[59] Donaldson, L., Nanayakkara, B., & Harrington, J. (2016). Wood Growth and Development. Encyclopedia of Applied Plant Sciences, 1, 203–210. doi:10.1016/B978-0-12-394807-6.00114-3.

[60] Hu, X., Guo, H., Gholizadeh, M., Sattari, B., & Liu, Q. (2019). Pyrolysis of different wood species: Impacts of C/H ratio in feedstock on distribution of pyrolysis products. Biomass and Bioenergy, 120, 28–39. doi:10.1016/j.biombioe.2018.10.021.

[61] Wijitkosum, S., & Sriburi, T. (2023). Aromaticity, polarity, and longevity of biochar derived from disposable bamboo chopsticks waste for environmental application. Heliyon, 9(9), e19831. doi:10.1016/j.heliyon.2023.e19831.

[62] Spokas, K. A., Cantrell, K. B., Novak, J. M., Archer, D. W., Ippolito, J. A., Collins, H. P., Boateng, A. A., Lima, I. M., Lamb, M. C., McAloon, A. J., Lentz, R. D., & Nichols, K. A. (2012). Biochar: A Synthesis of Its Agronomic Impact beyond Carbon Sequestration. Journal of Environmental Quality, 41(4), 973–989. doi:10.2134/jeq2011.0069.

[63] Bakshi, S., Banik, C., & Laird, D. A. (2020). Estimating the organic oxygen content of biochar. Scientific Reports, 10(1), 13082. doi:10.1038/s41598-020-69798-y.

[64] Sriburi, T. (2013). Biochar Production for Soil Amendment at Huay Sai Royal Development Study Center and Pa-deng Biochar Research Center (PdBRC), Petchburi Province, Thailand. International Conference on Agriculture Science and Environment Engineering (ICASEE 2013), Beijing, China.

[65] Lehmann, J., & Joseph, S. (2024). Biochar for environmental management: Science, Technology and Implementation. Routledge, London, United Kingdom. doi:10.4324/9781003297673.